Food Hydrocolloids 45 (2015) 102–110

Contents lists available at ScienceDirect

Food Hydrocolloids

journal homepage: www.elsevier.com/locate/foodhyd

Effect of high intensity ultrasound on physicochemical and functional properties of aggregated soybean β-conglycinin and glycinin

Hao Hu [a, b, c], Imelda W.Y. Cheung [b], Siyi Pan [a, c, *], Eunice C.Y. Li-Chan [b, **]

[a] College of Food Science and Technology, Huazhong Agricultural University, Wuhan, Hubei 430070, PR China
[b] The University of British Columbia, Faculty of Land and Food Systems, Food Nutrition and Health Program, 2205 East Mall, Vancouver, British Columbia, Canada V6T 1Z4
[c] Key Laboratory of Environment Correlative Dietology, Huazhong Agricultural University, Ministry of Education, PR China

ARTICLE INFO

Article history:
Received 17 December 2013
Accepted 6 November 2014
Available online 18 November 2014

Keywords:
High intensity ultrasound
Soy β-conglycinin
Soy glycinin
Emulsifying properties
Physicochemical properties

ABSTRACT

The effects of high intensity ultrasound treatment (HUS; 20 kHz at 400 W for 5, 20 or 40 min) on aggregated soybean β-conglycinin (7S) and glycinin (11S) fractions were investigated in this study. HUS decreased turbidity and particle size of 7S in 0.05 M Tris–HCl buffer at pH 7.0, while it increased surface hydrophobicity (H_0), solubility, emulsifying activity (EAI) and emulsion stability (ESI). Similarly, HUS of soybean 11S decreased turbidity while increasing EAI but it had minimal effects on particle size and ESI. The SH groups of both 7S and 11S fractions decreased after HUS. HUS did not change 7S or 11S secondary structure, but it slightly increased the percentage of high molecular-weight aggregates under non-reducing SDS-PAGE, and changed the microenvironment of aromatic and aliphatic side chains as observed by Raman spectroscopy of freeze-dried samples. These findings on physicochemical changes of 11S and especially of 7S proteins induced by HUS treatment may contribute to improved applications of soy proteins in food products.

1. Introduction

Ultrasonic technology, which is based on mechanical waves at a frequency above the threshold of human hearing (>16 kHz) is attracting much attention of food industry (Jambrak, Lelas, Mason, Kresic, & Badanjak, 2009). Sonication technology can be classified into two types: high frequency low intensity (100 kHz–1 MHz, power < 1 W/cm^2) and low frequency high intensity (16–100 kHz, power 10–1000 W/cm^2). The former is often used for non-destructive analysis, while the latter is relatively new in food industry and is widely used to alter food properties (Zheng & Sun, 2006). The effects of high intensity ultrasound (HUS) on liquid systems are mainly due to the cavitation phenomenon and micro-streaming currents (Zheng & Sun, 2006). During sonication, cavitation bubbles are formed, which grow over a few cycles and violently collapse, resulting in extreme temperatures (5000 K), pressures (1000 atm), very high shear energy waves and turbulence in the cavitation zone (Chandrapala, Zisu, Palmer, Kentish, & Ashokkumar, 2011; Gülseren, Güzey, Bruce, & Weiss, 2007). Moreover, the bubble size variation and the diffusion of gases into and out of the bubbles create micro-currents which further spread into the liquid (Zheng & Sun, 2006). Furthermore, highly reactive free radicals can be generated by HUS from water ($H_2O \rightarrow {}^{\bullet}H + {}^{\bullet}OH$), leading to chemical reactions (Gülseren et al., 2007).

Soy protein has been widely used in food industry because of its ability to improve texture while contributing to the nutritional and health benefits of protein-based foods (Kinsella, 1979; Nishinari, Fang, Guo, & Phillips, 2014; Tang, Chen, & Foegeding, 2011; Tang, Wang, Yang, & Li, 2009). Recently, several studies have found that HUS altered physicochemical properties resulting in improved functional properties of soy protein products, such as soy protein isolate (SPI) and soy protein concentrate (SPC). Tang et al. (2009) showed that HUS increased protein solubility and heat gelling property of commercial SPI. Similarly, Jambrak et al. (2009) found that HUS of SPC and SPI increased solubility, the specific surface area and emulsion activity index but it reduced the particle size of SPI and SPC. Changes in SH content, surface hydrophobicity and flow behavior of SPI by HUS were observed by Arzeni et al. (2011).

* Corresponding author. Key Laboratory of Environment Correlative Dietology, Huazhong Agricultural University, Ministry of Education, PR China. Tel.: +86 027 87283778; fax: +86 027 87288373.
** Corresponding author. Tel.: +1 604 822 6182; fax: +1 604 822 3959.
E-mail addresses: siyipan@yahoo.com.cn (S. Pan), eunice.li-chan@ubc.ca (E.C.Y. Li-Chan).

http://dx.doi.org/10.1016/j.foodhyd.2014.11.004
0268-005X/

Interestingly, Chen, Chen, Ren, and Zhao (2011) reported that HUS pretreatment increased the emulsifying properties of SPI hydrolyzates and Karki et al. (2009) reported that HUS pretreatment of soy flakes increased the SPI yield and altered the physical properties of isolated SPI. Moreover, our previous studies showed that HUS changed the structural, physicochemical and functional properties of commercial SPI (Hu, Wu, et al., 2013), especially improving the gelation properties of tofu-type gels (Hu, Fan, et al., 2013; Hu, Li-Chan, Wan, Tian, & Pan, 2013).

Among the four fractions (2S, 7S, 11S and 15S) of soy proteins as categorized by their sedimentation coefficients, the 7S (β-conglycinin) and 11S (glycinin) fractions are the principal components accounting for 65–80% of the total seed proteins (Jambrak et al., 2009). The 7S fraction, mainly β-conglycinin, is a trimer consisting of the non-covalently associated subunits α′, α and β (Fukushima, 2001). The diameter of the homotrimer is about 9.6 nm × 9.6 nm, and the thickness is about 4.4 nm (Chen & Ono, 2014; Maruyama et al., 2001). The 11S fraction, mainly glycinin, is a hexameric protein composed of A and B polypeptides linked by disulfide bridges (Fukushima, 2001), with dimensions of about 9.5 nm × 9.2 nm, and thickness is about 8 nm (Adachi et al., 2003). However, to the best of our knowledge, little is known about the effects of HUS treatment and freeze-drying on the structural and physicochemical properties of soy 7S and 11S fractions. Thus, in this study, we investigated the structural and physicochemical changes of 7S and 11S fractions as a function of HUS (400 W for 0–40 min), in order to provide some fundamental information on how HUS impacts the structures of 7S and 11S, influencing their physicochemical and functional properties, which may lead to improvements in the application of HUS in the soy protein industry.

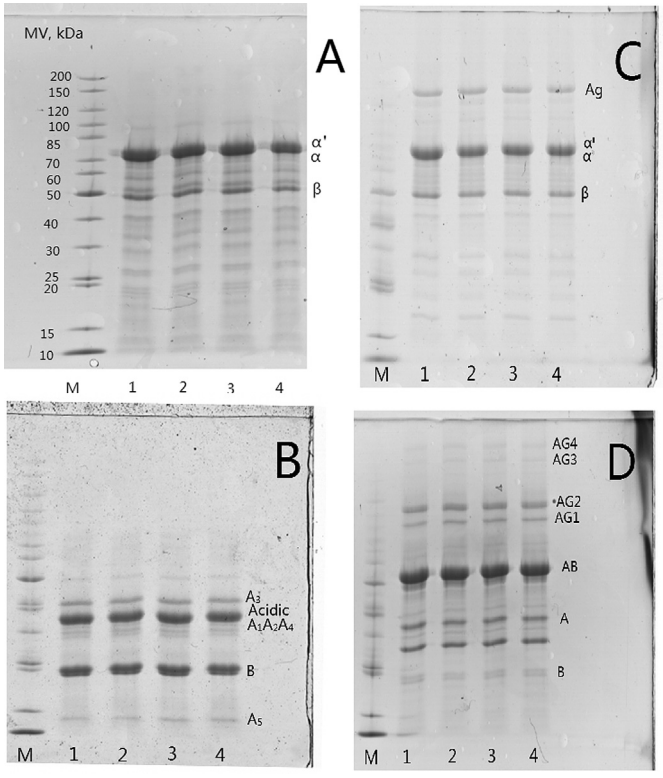

Fig. 1. Sodium dodecyl sulfate-polyacrylamide gel electrophoresis of high intensity ultrasound (HUS; 20 kHz at 400 W) treated β-conglycinin (7S) and glycinin (11S) fractions under reducing and non-reducing conditions. A: 7S fractions under reducing condition; B: 11S fractions under reducing condition; C: 7S fractions under non-reducing condition; D: 11S fractions under non-reducing condition. For all A, B, C and D patterns, Lane M: marker; Lane 1: non-HUS treated samples; Lane 2: 5 min HUS treated samples; Lane 3: 20 min HUS treated samples; Lane 4: 40 min HUS treated samples.

2. Material and methods

2.1. Materials

Defatted 7B soy flour, which is a "minimally heat processed product that most closely resembles native raw soybeans", was a gift from the Archer Daniels Midland (ADM) company (Decatur, IL, USA). 5,5′-Dithiobis-(2-nitrobenzoic acid) (DTNB) was purchased from Sigma Chemical Co. (St. Louis, MO, USA). 1-Anilino-8-naphthalene-sulfonate (ANS) was obtained from Sigma–Aldrich (Buchs, Switzerland). Pure corn oil was obtained from ACROS ORGANICS (Geel, Belgium). Other chemicals used in this study were of analytical grade.

2.2. Preparation of 7S and 11S fractions

7S and 11S fractions were isolated from 7B soy flour according to the method of Nagano, Hirotsuka, Mori, Kohyama, and Nishinari (1992). The obtained 7S and 11S fractions were washed twice with distilled water, adjusted to pH 7.5 with 1 N NaOH, and then freeze-dried. The SDS-PAGE profiles of the 7S and 11S fractions are shown in Fig. 1. The isolated 7S and 11S fractions contained 3.1% and 1.3% salt, respectively, based on the determination of conductivity with NaCl solution as a standard curve.

2.3. Preparation of high intensity ultrasound treated 7S and 11S fractions

7S and 11S dispersions (3%, w/v) were prepared by adding distilled water into protein powder and then gently stirring for 2 h. Samples were treated at 20 kHz at 400 W for 0, 5, 20 or 40 min using an ultrasound processor model JY92-2D (NingBo Scientz Biotechnology Co. Ltd., Ningbo, Zhejiang, China) with a 0.636 cm diameter titanium probe, as described in detail in our previous paper (Hu, Li-Chan, et al., 2013). The ultrasonic intensity, which was analyzed according to Hu, Fan, et al. (2013) using the method of Jambrak et al. (2009), was 105–110 W/cm^2 in this study. After ultrasound treatments, all samples were lyophilized and then stored at 4 °C in air tight containers. The whole samples were used to carry out the following experiments.

2.4. Sodium dodecyl sulfate-polyacrylamide gel electrophoresis

Sodium dodecyl sulfate polyacrylamide gel electrophoresis (SDS-PAGE) was carried out in duplicate under reducing and non-reducing conditions. For reducing SDS-PAGE, 80 μL of sample (2 mg/mL) was mixed with 20 μL of 10% SDS, 2 μL of 2-mercaptoethanol and 1 μL of 1% w/v bromophenol blue. For non-reducing SDS-PAGE, 2-mercaptoethanol was not added. The mixtures were boiled for 20 min, and then centrifuged for 5 min. The SDS-PAGE process was performed according to the PhastSystem™ Separation Technique (GE Healthcare, Uppsala, Sweden) with PhastGel® gradient 10–15 and Fisher BioReagents EZ-Run *Rec* protein ladder (Fisher Scientific, Ottawa, ON, Canada). The gels were analyzed using Image Scanner III and Image Quant TL software (GE Healthcare, Uppsala, Sweden).

2.5. Particle size determination

Because soymilk has a pH near neutrality (Liu & Chang, 2004), the 7S and 11S fractions were reconstituted in pH 7.0 (0.05 M Tris–HCl buffer containing 0.01% sodium azide) buffer, hereinafter

referred to as "standard buffer". Due to the large difference in particle sizes between 7S and 11S fractions in the standard buffer, their mean particle diameter was measured using two different instruments. For 7S fractions, ZS Zetasizer Nano (Malvern Instrument Ltd, UK) that provides 0.3 nm–10.0 μm diameter measurement range was used. The average hydrodynamic size of particles in solution was determined according to the Stokes–Einstein equation and determinations were conducted in triplicate. For 11S fractions, Mastersizer 2000 equipped with a Hydro 2000 MU dispersion unit (Malvern Instruments Ltd., UK), which provides 0.02–2000 μm diameter measurement range was used. The particle size was described by the volume-weighted mean diameter (D_{43}) and determinations were conducted in duplicate.

2.6. Protein solubility

The protein solubility of samples was determined by modifying the method of Jambrak et al. (2009). Lyophilized samples (2 mg/mL) were dispersed in pH 7.0 standard buffer. The mixtures were stirred for 90 min at room temperature, and then centrifuged at 20 000 *g* for 15 min at 25 °C. The protein concentration in the samples before centrifugation and in the supernatants after centrifugation was determined by the bicinchoninic acid protein assay kit (Thermo Scientific, Rockford, IL, USA), using bovine serum albumin as standard. All determinations were conducted in triplicate. Protein solubility (%) was calculated as 100*(protein content of the supernatant)/(total protein content before centrifugation).

2.7. Turbidity measurement

The turbidity of 7S and 11S samples was determined by modification of the method of Martini, Potter, and Walsh (2010). Soy protein dispersions were prepared in standard buffer to the appropriate concentration (2% w/v for 7S and 0.25% w/v for 11S), and stirred at room temperature for 1 h. Absorbance of the dispersions at 600 nm (Model UV-1700 Spectrophotometer, Shimadzu Co., Kyoto, Japan) was measured to represent turbidity. All determinations were conducted in triplicate.

2.8. Circular dichroism spectra measurement

Circular dichroism (CD) spectral data were collected in the far-UV range (260–185 nm) with a CD spectropolarimeter (Jasco J-810, Jasco Corp., Tokyo, Japan) in a 0.2 cm quartz CD cuvette at 20 °C. Freeze-dried soy protein samples were prepared as 0.1 mg/mL solutions in 0.01 M sodium phosphate buffer (pH 7.0). The scan rate, response, and bandwidth were 50 nm/min, 4 s and 1.0 nm, respectively. Three scans were averaged to obtain one spectrum. The proportion of four secondary structures (α-helix, β-sheet, β-turn, unordered) was calculated using the CDPro software from Sreerama's website (http://lamar.colostate.edu/~sreeram/CDPro/). Duplicate analyses were performed.

2.9. Fourier transform infrared spectroscopy

The freeze-dried HUS treated and non-HUS treated 7S and 11S samples were analyzed by Fourier transform infrared spectroscopy (FT-IR) using a Perkin–Elmer Spectrum 100 FTIR spectrometer (Perkin–Elmer, Waltham, MA, USA). The FT-IR spectra were recorded with 64 scans at 4 cm^{-1} resolution from 1700 to 1600 cm^{-1}. The parameters of deconvolution were set with a gamma value of 2.5 and a smoothing length of 70%.

2.10. FT-Raman spectroscopy

Due to the poor signal-to-noise ratio of the spectra of aqueous samples, FT-Raman spectra were only collected on the dry samples. Freeze-dried samples were ground by a mortar and pestle, and then placed into glass NMR tubes for FT-Raman spectrum measurement. The FT-Raman spectral data were collected on a Nexus 670 FT-Raman spectrometer equipped with CaF_2 beam splitter and Ge detector (Thermo Nicolet Corp, Madison, WI, USA) as described by Moon and Li-Chan (2007), except for an increase in scan number from 512 to 1024. Spectral data processing, including baseline correction, normalization to the intensity of phenylalanine peak at 1003 ± 1 cm^{-1} and Raman difference spectra calculation, was performed using OMNIC (Thermo Fisher scientific, Madison, WI, USA) and Perkin–Elmer Spectrum version 10.00.00 software.

2.11. Sulfhydryl contents

7S and 11S samples were prepared in pH 8.0 buffer B (0.086 M Tris–0.09 M glycine 4 mM Na_2EDTA) or buffer BSU (buffer B containing 0.5% sodium dodecyl sulfate and 8 M urea) at a protein concentration of 0.2%. After stirring for 2 h at room temperature, the free (in buffer B) or total (in buffer BSU) sulfhydryl (SH) contents of the 7S and 11S samples were determined using Ellman's reagent DTNB by modification of the method of Shimada and Cheftel (1988), as previously described (Hu, Fan, et al., 2013). All determinations were conducted in triplicate.

2.12. Surface hydrophobicity

Soy protein samples were dissolved in standard buffer to obtain protein concentrations ranging from 0.005 to 0.25 mg/mL. Surface hydrophobicity (H_0) of whole samples was determined in the absence of SDS using ANS as fluorescence probe according to the method of Hayakawa and Nakai (1985). All determinations were conducted in triplicate.

2.13. Emulsifying tests

Emulsifying activity index (EAI) and emulsion stability index (ESI) were measured according to the method of Pearce and Kinsella (1978) as modified by Cameron, Weber, Idziak, Neufeld, and Cooper (1991) and others (Tang, Sun, & Foegeding, 2011; Shen & Tang, 2012). Corn oil (1 mL) and 0.5% 7S or 11S solution in standard buffer (3 mL) were pipetted into a microchamber, attached to the Omni mixer (Model 17105, Omni International, Gainesville, VA, USA), then homogenized for 1 min at setting 7. Aliquots (50 μL) of the emulsion were taken from the bottom of the chamber immediately (time 0) and at subsequent time intervals, and diluted into 9.95 mL (200-fold) 0.3% SDS solution. The absorbance of the diluted solutions was measured at 500 nm. All determinations were conducted in triplicate. EAI was calculated as follows:

$$\mathrm{EAI}\left(\mathrm{m}^2/\mathrm{g}\right) = 2T\frac{A_0 \times \text{dilution factor}}{c \times \varphi \times 1 - \theta \times 10\,000}$$

where $T = 2.303$, A_0 = absorbance at time 0, dilution factor = 200, c = the weight of protein per unit volume (g/mL), φ (optical path) = 1 cm, and θ = the oil volume fraction (0.25).

ESI was represented by the time in minutes when the absorbance at 500 nm was half that of A_0, the initial absorbance at 500 nm of the emulsion when first formed.

2.14. Statistical analysis

Values given in the tables and figures are the means of duplicate or triplicates, and error bars indicate the standard deviation. Statistical significance of differences among means was evaluated by Duncan's test at $p < 0.05$. Statistical analysis was performed using SPSS software version 17.0.

3. Results and discussion

Fig. 1 shows the SDS-PAGE patterns of non-HUS treated and HUS treated 7S and 11S fractions under reducing (Fig. 1A and B) and non-reducing (Fig. 1C and D) conditions. Fig. 1A and C are the electrophoregrams for 7S, while Fig. 1B and D are the electrophoregrams for 11S. Under reducing conditions, bands at ~70 kDa were observed, corresponding to the molecular weights (MW) reported for α′ and α subunits, while bands near 50 kDa correspond to the β subunits of soy 7S globulin (Fig. 1A). Reducing SDS-PAGE of the 11S fraction resulted in bands with MWs of ~30 kDa and 20 kDa that were assigned to the acidic (A_1–A_5) and basic (B) polypeptide chains, respectively (Fig. 1B). Moreover, compared with 11S fraction, the 7S fraction exhibited lower turbidity (Table 2), smaller particle size (Table 2) and fewer SH groups (Fig. 3) as well as better emulsifying properties (Fig. 3), which were consistent with other previous reports (Bian et al., 2003; Thanh & Shibasaki, 1976; Wu, Murphy, Johnson, Fratzke, & Reuber, 1999; Zhang, Li, & Mittal, 2010).

3.1. Particle size, protein solubility and turbidity

Particle size of proteins is one of the numerous factors that influence the functional properties of soy proteins (Kinsella, 1979). The effects of HUS on the average hydrodynamic size (nm) of 7S fractions and volume-weighted mean diameter (μm) of 11S fractions are shown in Table 2. The sizes of native 7S and 11S globulins are around 10 nm (Fukushima, 2001; Nishinari et al., 2014). Thus, from the particle size data, it may be concluded that the proteins in the isolated soy fractions, especially 11S fractions, were aggregated in the standard buffer. The average hydrodynamic size of 7S decreased from 75.9 nm to 51.8 nm when treated by HUS for 40 min, which may be due to the dissociation of aggregates of 7S fractions caused by local extreme temperature, pressures and high shear energy waves and turbulence from cavitation phenomenon (Hu, Li-Chan, et al., 2013; Zhu & Yang, 2010). Moreover, the particle distribution of 7S was also changed by HUS (see Supplementary Fig. 1), but that of 11s was not (Supplementary Fig. 2). The volume-weighted mean diameter of 11S fractions increased from 228.7 μm to 241.2 μm during the first 20 min, and then decreased to 216.8 μm upon longer HUS; however, these changes were not significant at $p > 0.05$. Furthermore, the particle sizes of 11S were larger than 200 μm, indicating they were not appropriate for reliable analysis of protein solubility, surface hydrophobicity and CD spectra. Thus, the information of these parameters of 11S was excluded in this study.

Several studies have investigated the effect of sonication on particle size of different proteins and divergent findings were reported. For example, Jambrak et al. (2009), Arzeni et al. (2011) and our previous study (Hu, Fan, et al., 2013) found that HUS reduced the particle size of commercial SPI, SPC and whey protein concentrate. Furthermore, Zisu, Bhaskaracharya, Kentish, and Ashokkumar (2010) pointed out that pilot-scale ultrasonic treatments reduced particle size of whey protein. The reduction of the above protein particle size may be due to the cavitational forces of HUS exerted by the probe, micro-streaming and turbulent forces (Hu, Fan, et al., 2013). However, Arzeni et al. (2011) and Gülseren et al. (2007) found that mean diameters of egg white protein and native bovine serum albumin, respectively, increased after HUS treatment. These authors attributed the increasing particle size to the formation of small aggregates after HUS treatments. Moreover, Gordon and Pilosof (2010) found that when sonication was conducted at ambient temperature, the particle size was reduced (from 0.7 μm to 0.2 μm) for whey protein isolate at 7.5%, while when sonication was conducted with heating, the particle size was reduced for whey protein isolate at 7.5% and did not change at 9% but was greatly increased at 12% concentration.

Protein solubility is determined as the protein content in the supernatant after centrifugation at 20 000 *g*. Smaller mean diameters of the particles would be expected to result in less protein in the pellet after centrifugation and therefore higher solubility. Moreover, smaller particle size means greater surface area and increased protein-water interactions. Thus, protein solubility and particle size are usually inversely related. The 7S fraction showed good solubility (Table 2) in the standard buffer, which was consistent with a previous study (Maruyama et al., 1999). Moreover, the results in Table 2 show that the protein solubility of 7S fraction increased from 85% to 93% while particle size decreased with increasing HUS time. Various researchers (Arzeni et al., 2011; Chen et al., 2011; Hu, Wu, et al., 2013; Jambrak et al., 2009; Karki et al., 2009; Tang et al., 2009) found that ultrasound improved protein solubility of SPI. The protein solubility of 11S fraction could not be determined reliably due to its large particle size (more than 200 μm) and tendency to precipitate even before centrifugation for protein solubility analysis.

Table 1
Band intensity (%) observed for 7S and 11S fractions by SDS-PAGE under non-reducing conditions.

Band intensity of 11S (%)								
HUS time	AG4	AG3	AG2	AG1	AB	A	B	Others
0 min	**0.44 ± 0.33B**	**0.41 ± 0.04C**	8.52 ± 0.71A	4.05 ± 0.57A	60.69 ± 2.25A	10.46 ± 0.65A	2.25 ± 0.28A	13.19 ± 0.26A
5 min	**1.13 ± 0.04A**	**0.88 ± 0.08AB**	8.74 ± 0.66A	4.66 ± 0.57A	58.73 ± 0.26A	10.19 ± 0.48A	1.66 ± 0.06A	14.02 ± 0.91A
20 min	**1.16 ± 0.17A**	**1.04 ± 0.13AB**	9.35 ± 0.13A	4.61 ± 0.65A	59.01 ± 0.56A	9.48 ± 0.32A	1.84 ± 0.08A	13.54 ± 0.50A
40 min	**1.19 ± 0.04A**	**1.16 ± 0.04A**	8.71 ± 0.53A	4.63 ± 0.37A	59.48 ± 2.04A	9.12 ± 0.80A	1.81 ± 0.57A	13.92 ± 0.48A
Band intensity of 7S (%)								
HUS time		Ag		α′ + α		β		Others
0 min		**6.19 ± 0.35b**		41.81 ± 5.32a		15.30 ± 0.10a		36.70 ± 5.08a
5 min		**7.58 ± 0.40a**		40.76 ± 2.43a		14.89 ± 0.68a		36.77 ± 2.69a
20 min		**7.45 ± 0.57a**		44.66 ± 3.32a		17.35 ± 2.64a		30.55 ± 1.23a
40 min		**7.60 ± 0.35a**		43.68 ± 3.75a		16.21 ± 0.12a		32.53 ± 4.24a

Bold numbers indicate significant difference at $p < 0.05$ after HUS treatments.
Different letters indicate significant difference among treatments (HUS time) for the bands of each sample (11S or 7S) at $p < 0.05$ using Duncan's test.

Table 2
Effect of high intensity ultrasound treatments (20 kHz at 400 W for 0, 5, 20 or 40 min) on particle size, protein solubility and turbidity of β-conglycinin (7S) and glycinin (11S) fractions.

	Particle size		Protein solubility (%)		Turbidity (Abs_{600})	
	7S (nm)	11S (μm)	7S	11S	2% 7S	0.25% 11S
0 min	75.9 ± 4.6a	228.7 ± 12.9a	85 ± 0d	N.D.	0.602 ± 0.003a	1.355 ± 0.015a
5 min	57.2 ± 0.4b	229.6 ± 6.3a	88 ± 1c	N.D.	0.158 ± 0.001b	0.928 ± 0.019b
20 min	50.4 ± 0.7c	241.2 ± 11.0a	91 ± 1b	N.D.	0.154 ± 0.001c	0.881 ± 0.022c
40 min	51.8 ± 0.5c	216.8 ± 2.4a	93 ± 2a	N.D.	0.147 ± 0.001d	0.789 ± 0.025d

Different letters (a, b, c, d) within a column indicate significant difference among treatments at $p < 0.05$ using Duncan's test.
N.D., not determined (the protein solubility of 11S fraction could not be determined reliably due to its large particle size and tendency to precipitate even before centrifugation for protein solubility analysis).

11S samples were much more turbid than 7S samples thus lower concentrations of 11S than 7S were prepared for measurement of turbidity. HUS treatments decreased the turbidity of both 2% (w/v) 7S and 0.25% (w/v) 11S samples, from 0.602 and 1.355 to 0.147 and 0.789, respectively, as a function of the HUS time (0–40 min) (Table 2). Madadlou, Mousavi, Emam-Djomeh, Ehsani, and Sheehan (2009) observed that ultrasonic treatment (35 and 135 kHz) resulted in a decrease in the turbidity of casein solutions and diameter of particles at any given pH value ranging from 6.35 to 11.4. Smaller particle size could similarly be considered as one reason for the decrease in protein solution turbidity of 7S fraction as a function of HUS time (0–40 min) (Table 2). However, the lower turbidity of 11S fraction after HUS was not consistent with the particle size changes (Table 2). In this study, changes in tertiary and quaternary structure of non-aggregated proteins (Martini et al., 2010), as well as changes in the particle size distribution may have resulted in the lower turbidity of soy proteins after HUS treatment. Furthermore, from Table 2, it was observed that the decrease in turbidity by HUS was much greater for 7S than for 11S. For example, the turbidity of non-HUS treated 7S was decreased over 4-fold after 40 min HUS, while that of 11S was decreased less than 2-fold. The reason might be due to HUS-induced reduction of the particle size of 7S but not of 11S.

In order to further understand the effect of HUS on physicochemical properties of 7S and 11S fractions, some parameters referring to protein structure were investigated.

3.2. Secondary structure

The effects of HUS on the circular dichroism (CD) spectra of 7S are shown in Supplementary Fig. 3A. The estimated secondary structure of non-HUS treated globulins was 3.4% α-helix, 39.7% β-sheet, 18.0% β-turn and 38.9% unordered for 7S fraction. Duncan's test showed that HUS did not significantly change the secondary structure of 7S fractions. Moreover, the deconvoluted FT-IR spectra of 7S and 11S fractions in the amide I region are shown in Supplementary Fig. 3B and C, respectively. Similar spectra were observed, regardless of HUS time. Similarly, from Fig. 2A and B, it was observed that HUS treatments did not change the amide I and amide III regions assigned to vibrational modes associated with secondary structure of 7S and 11S proteins. The above data suggested that HUS of 7S and 11S did not lead to significant disruption of the hydrogen bonds between C=O and H–N groups on the polypeptide backbone. These results are consistent with literature reporting that cavitation shearing might disrupt tertiary structure but leave most of the secondary structural elements intact (Stathopulos et al., 2004). Stathopulos et al. (2004) found that significant secondary structural change upon ultrasonic-induced aggregation was not observed for proteins with high levels of β-structure and low levels of α-structure (Tm0979, Cu/Zn superoxide dismutase and hisactophilin), while proteins with high α-helical content (bovine serum albumin, myoglobin and lysozyme) underwent an increase of β-structure. Our results are consistent with those of Stathopulos et al. (2004), since CD analysis of the 7S proteins in this study indicated high levels of β-structure and low levels of α-helical structure, which consequently might be expected to show minimal changes after HUS. Conflicting results have been reported in other studies on the effect of ultrasound on secondary structures of proteins. For example, Chandrapala et al. (2011) and Gülseren et al. (2007) observed that sonication resulted in an increase in the α-helix component and a decrease in the β-sheet and turn components of β-lactoglobulin and bovine serum albumin solutions. A reduction of unordered structure was found in bovine serum albumin (Gülseren et al., 2007) while our previous study (Hu, Wu, et al., 2013) found that higher sonication power combined with longer time could increase the random coil and β-turn components of SPI. The discrepancy between these studies might be due to differences in the proteins and sonication conditions used.

3.3. Tertiary and quaternary structure

FT-Raman spectroscopy, which provides information on the microenvironment and chemistry of amino acid side chains of the polypeptide backbone, is widely used in food protein analysis (Li-Chan, Ismail, Sedman, & van de Voort, 2002). The microenvironment of aliphatic amino acid residues was investigated by monitoring changes in the spectra at 1450 cm^{-1} (C–H_2 bending), 1465 cm^{-1} (C–H bending) or 2935 cm^{-1} (C–H stretching) (Table 3 and Fig. 2). HUS resulted in changes in the normalized intensity values of FT-Raman spectral peaks assigned to various amino acid side chains (Table 3 and Fig. 2C and D). HUS of 7S and 11S caused decreases in the intensity of the peak near 1450 cm^{-1} and the shoulder at 1465 cm^{-1} and an increase in the intensity near 2933 cm^{-1}, suggesting changes of the polarity of the microenvironment around hydrocarbon chains (Li-Chan et al., 2002). The intensity of the aromatic or unsaturated = C–H stretching band of 7S and 11S near 3060 cm^{-1} also increased after HUS treatments (Table 3 and Fig. 2). One might speculate that the changes in intensity of the vibrations of the C–H_2 bending, C–H bending, C–H stretching and = C–H stretching bands near 1450, 1465, 2933 and 3060 cm^{-1}, respectively, demonstrate changes in the environment of C–H groups which may be related to hydrophobic interactions and conformational changes arising from the HUS treatment.

Free sulfhydryl (SH) groups are those SH groups that are located on the surface of the protein and are readily accessible to react with Ellman's reagent. For detecting total SH groups, SDS and urea were added to the buffer to expose SH groups that were buried within the protein structure. Many researches had been carried out to study the SH groups of soy proteins, with a range of results being reported. For example, the reported contents of free SH groups of 7S fraction (assumed molecular weight 150 000) were in the range of 2.3–9.5 μmol/g protein (Hou & Chang, 2004a,b; Tezuka, Yagasaki, &

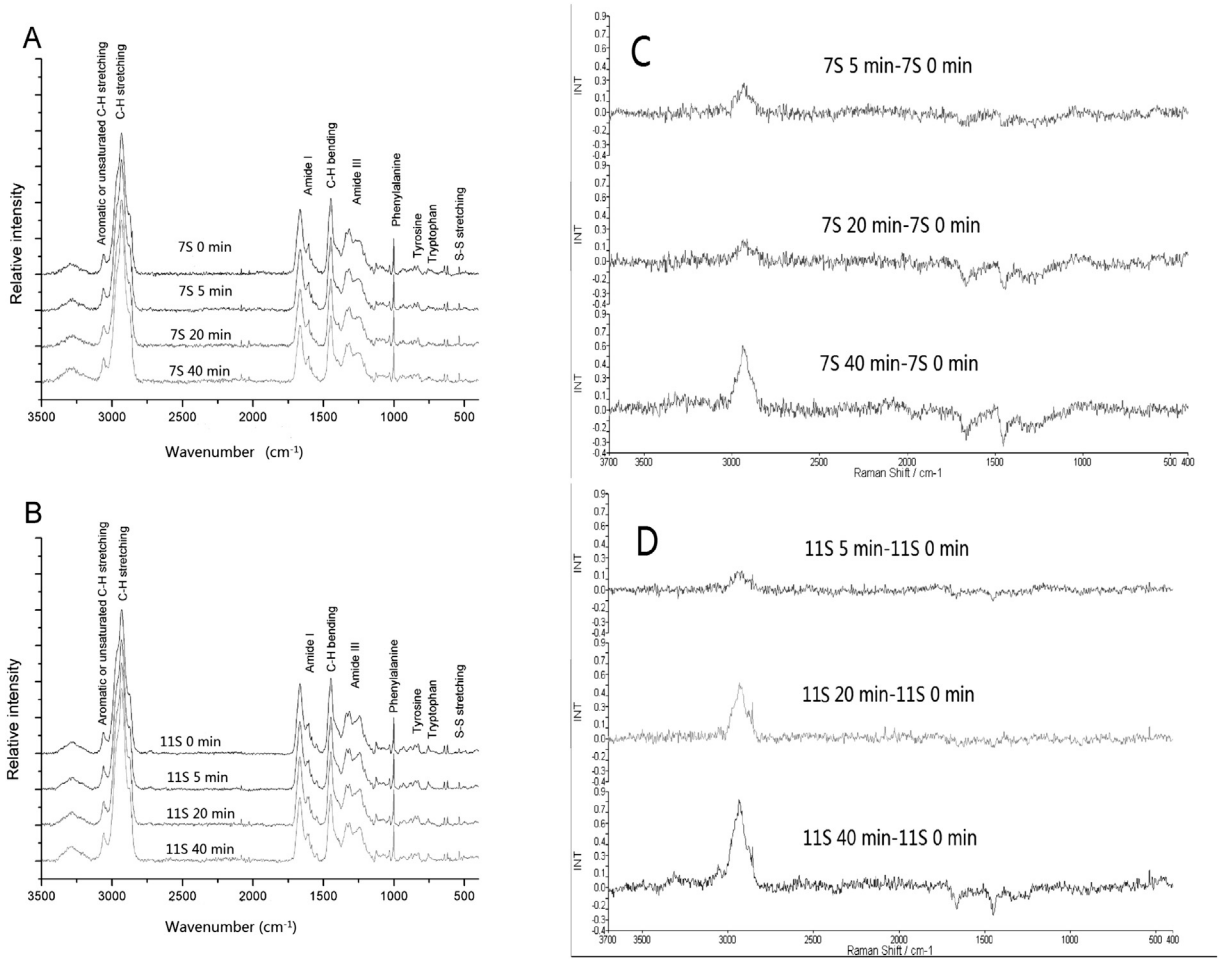

Fig. 2. FT-Raman spectra of freeze-dried high intensity ultrasound (HUS; 20 kHz at 400 W) treated β-conglycinin (7S) and glycinin (11S) fractions. A: FT-Raman spectra of 7S fraction treated by HUS at 0, 5, 20 or 40 min. B: FT-Raman spectra of 11S fraction treated by HUS at 0, 5, 20 or 40 min. C: Difference spectra resulting from subtraction of spectrum for untreated (0 min) 7S from the spectra for 5, 20 or 40 min HUS-treated 7S. D: Difference spectra resulting from subtraction of spectrum for untreated (0 min) 11S from the spectra for 5, 20 or 40 min HUS-treated 11S.

Ono, 2004; Wu et al., 1999; Zhang et al., 2010), while reported contents of free SH groups of 11S fraction (assumed molecular weight 320 000) were in the range of 0–32.2 μmol SH/g protein (Faris, Wang, & Wang, 2008; Hoshi & Yamauchi, 1983). The different contents reported may be due to different soy cultivars, denaturants, solubilization conditions (Shimada & Cheftel, 1988), soybean storage conditions (Hou & Chang, 2004a, 2004b; Hou et al., 2004a, 2004b) and protein extraction conditions (Wu et al., 1999). Fig. 3B shows that free SH-groups of 7S and 11S fractions decreased from 12.6 and 19.7 μmol SH/g protein to 7.72 and 12.0 μmol SH/g protein, respectively, after 40 min HUS treatments. Besides, total SH-groups of 7S and 11S fractions decreased from 14.2 and 22.3 μmol SH/g protein to 9.4 and 12.1 μmol SH/g protein, respectively, after 40 min HUS treatments (Fig. 3B). Similarly, Gülseren et al. (2007) also showed that the content of free SH groups in bovine serum albumin decreased with increasing sonication time. According to Gülseren et al. (2007), ultrasonic wave can generate highly reactive free radicals from water molecules ($H_2O \rightarrow {}^{\bullet}H + {}^{\bullet}OH$), which can react to produce hydrogen peroxide in the gas phase of the cavities. The hydrogen peroxide may oxidize susceptible free-SH groups to form S–S bonds, resulting in the decrease of free-SH groups (Gülseren et al., 2007). In contrast, our

Table 3
Normalized intensity values at selected regions of the Fourier transform Raman spectra of high intensity ultrasound (HUS; 20 kHz at 400 W for 0, 5, 20 or 40 min) treated β-conglycinin (7S) and glycinin (11S) fractions.[a]

Band assignment [wavenumber (cm^{-1})]	Normalized peak intensity							
	7S0	7S5	7S20	7S40	11S0	11S5	11S20	11S40
SS of cystine [538 cm^{-1}]	0.22	0.19	0.26	0.25	0.13	0.21	0.24	0.28
Tryptophan indole ring [756–758 cm^{-1}]	0.17	0.11	0.11	0.15	0.22	0.22	0.20	0.21
Aliphatic residues C–H bending [1446–1448 cm^{-1}]	2.12	2.04	1.88	1.85	2.11	2.02	2.05	1.87
Aliphatic residues C–H stretching [2931–2933 cm^{-1}]	3.94	4.20	4.07	4.52	4.01	4.17	4.54	4.81
Aromatic or unsaturated C–H stretching [3057–3062 cm^{-1}]	0.56	0.62	0.56	0.68	0.60	0.66	0.67	0.79

[a] 7S0: non-HUS treated 7S protein; 7S5, 7S20 and 7S40: 7S protein treated by HUS for 5, 20 and 40 min, respectively; 11S0: non-HUS treated 11S protein; 11S5, 11S20 and 11S40: 11S protein treated by HUS for 5, 20 and 40 min, respectively.

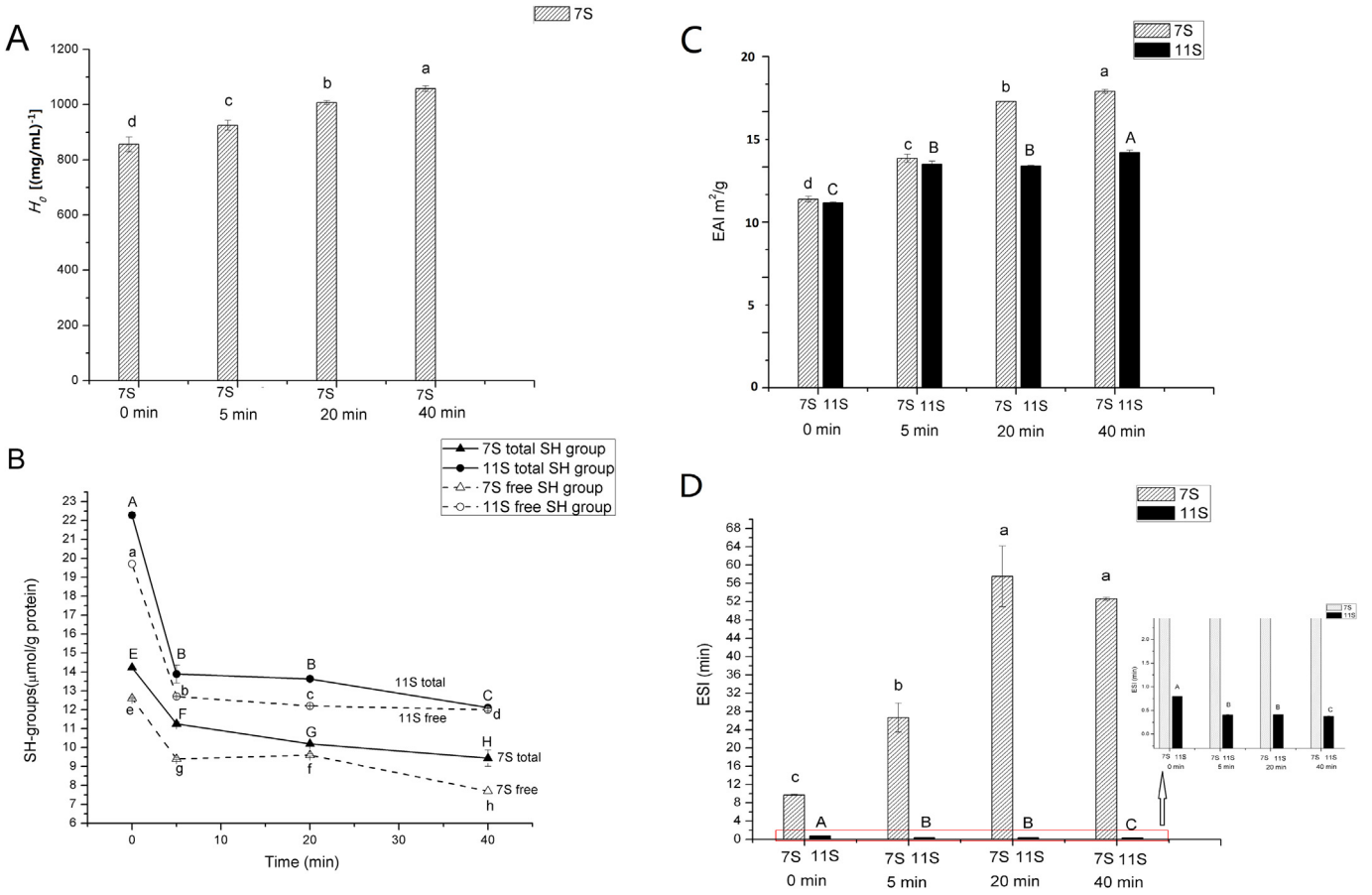

Fig. 3. Effect of high intensity ultrasound (HUS; 20 kHz at 400 W for 0, 5, 20 or 40 min) on A) surface hydrophobicity (H_0), B) free (—△— for 7S, —○— for 11S) or total (—▲— for 7S, —●— for 11S) SH groups, C) emulsifying activity index (EAI) and D) emulsion stability index (ESI) of 7S (hatched bars) and 11S (black bars) fractions. Different lower case letters (a, b, c, …) or upper case letters (A, B, C, …) indicate significant difference for 7S or 11S samples, respectively, at $p < 0.05$ using Duncan's test.

previous studies (Hu, Li-Chan, et al., 2013; Hu, Wu, et al., 2013) found that HUS increased the free SH-groups of commercial SPI with increasing HUS time. The contradictory results between the isolated soy globulins in this study and the commercial SPI in our previous studies might be attributed to the differences in structural properties of the protein molecules due to the isolation or production processes. Specifically, in this study, we produced 7S and 11S fractions from soy flour that has been minimally heat processed and most nearly resembles the native defatted portion in raw soybeans as raw material, and by using an isolation method with no reducing agent added (Nagano et al., 1992). However, during the production of commercial SPI, there are some steps, such as deactivation of enzymes at 85 °C, toasting and spray drying, which could result in the denaturation of soy protein, thus changing the native protein structure (Moon & Li-Chan, 2007).

The intensity of the S—S stretching band around 538 cm^{-1} was increased by HUS of soy proteins, especially the 11S fraction, the intensity of which increased from 0.13 to 0.28 after 40 min of HUS treatment (Table 3 and Fig. 2). It may be inferred that SH groups were oxidized to S—S bonds possibly by hydrogen peroxide formed from the radicals produced by HUS effect on water molecules (Gülseren et al., 2007).

In order to further investigate the formation of S—S bonds of 7S and 11S fractions after HUS, SDS-PAGE of the samples was carried out under non-reducing conditions. HUS slightly increased ($p < 0.05$) the percentage of high molecular-weight aggregates under non-reducing SDS-PAGE (Table 1). For 7S (Fig. 1C), the Ag aggregates (MW around 150 kDa) could be formed through intermolecular S—S bonds from α′ or α subunits (MWs around 70 kDa), because each of the α′ or α subunits possesses one —SH, while the β subunit does not possess any (Fukushima, 2001). The band intensity % of Ag increased significantly when been treated by HUS for 5 min or longer time (Fig. 1C and Table 1). For 11S (Fig. 1D and Table 1), it was observed that the intensities of AG3 and AG4 in lanes 2, 3 and 4 were significantly higher ($p < 0.05$) than those in lane 1. The band intensity % of AG3 and AG4 increased from 0.41% and 0.44% to 0.88% and 1.13%, respectively, at 5 min HUS and then remained unchanged at longer sonication time (Table 1). The above results indicated that intermolecular S—S bonds might be formed in 7S and 11S fractions after HUS, although the amount of intermolecular S—S bonds could be minor. Even though the intensity of Ag aggregate bands increased, the average particle size of 7S was reduced after HUS. The reason could be due to that HUS changed the particle distribution of 7S fraction. As shown in Supplementary Fig. 1, non-sonication treated 7S had three peaks at 12.18 nm, 70.89 nm and 2780 nm, of which the peak at 70.89 nm was a dominant peak. Sonication of 7S reduced the number of peaks into two, at 29.39 nm and 2780 nm, with the dominant peak being at 29.39 nm. It was obvious that sonication reduced the particle size of the dominant peak (from 70.89 to 29.39 nm), which contributed most to the reduction of average particle size. On the other hand, the increase of Ag aggregate bands might be correlated to the slight increase of the peak at 2780 nm.

Protein surface hydrophobicity (H_0), which is closely related to functional properties, is an index of the content of hydrophobic groups on the surface of a protein molecule in contact with the

polar aqueous environment. According to the previous studies of H_0 using ANS probe, sonication increased H_0 of several proteins, such as commercial SPI (Arzeni et al., 2011; Chen et al., 2011; Hu, Li-Chan, et al., 2013; Hu, Wu, et al., 2013), whey protein concentrate and egg white powder (Arzeni et al., 2011). In this study, the surface hydrophobicity (H_0) of 7S fraction progressively increased with increasing time of HUS from 856 to 1060 $(mg/mL)^{-1}$ after 40 min HUS (Fig. 3A), which was similar to the aforementioned studies. One reason for the increase of H_0 of 7S after HUS might be denaturation of the protein, which exposed some hydrophobic regions of 7S globulin from the interior of molecules to the surface. Since the particle size of 7S fraction decreased (Table 2) after HUS treatments, another possible reason for the increase of 7S H_0 after HUS was that the cavitation phenomenon dissociated the 7S aggregates, in other words, HUS may have reduced the intermolecular associations, leading to more hydrophobic regions being exposed to the solvent environment.

3.4. Emulsifying properties

The ability of proteins to assist in the formation and stabilization of emulsions is of critical importance for many applications such as frozen desserts, salad dressings, comminuted meats, mayonnaise, cake batters, milks and coffee whiteners (Kinsella, 1979). These emulsifying properties depend upon the molecular flexibility and stability of the protein structure (such as tertiary and quaternary structure) (Kinsella, 1979). Given the changes in physicochemical and structural changes of 7S and 11S fractions induced by HUS, its effect on emulsifying properties was further investigated.

Emulsifying activity index (EAI) of 7S and 11S fractions increased from 11.4 and 11.2 m^2/g to 17.9 and 14.2 m^2/g, respectively, with increasing HUS time to 40 min (Fig. 3C). Similarly, Jambrak et al. (2009) reported that HUS increased EAI of SPI and SPC, while Chen et al. (2011) found that the droplet size of emulsions was reduced when soy proteins were pretreated by HUS. Partial denaturation of the tertiary and quaternary structure and formation of a more disordered structure that could provide the protein a better potential to adsorb at the oil–water interface, were speculated to lead to an increase in EAI (Jambrak et al., 2009).

Emulsion stability index (ESI) of 7S increased from 9.7 min to 57.5 or 52.6 min after HUS treatment for 20 or 40 min respectively, while that of 11S decreased from 0.80 to 0.38 min after 40 min HUS (Fig. 3D). The stabilization of emulsified droplets is usually achieved by formation of a membrane of film around the droplets by protein (Kinsella, 1979). The best emulsion stability index (ESI) occurs for proteins that can unfold at the interface, interact with each other to form a stable film at the interface and stabilize the oil droplets from coalescence. Protein solubility is closely correlated with emulsion stability, influencing the protein migration to, adsorption at and rearrangement at the oil droplets' interface. Moreover, in oil–water systems, the proteins become unfolded, exposing hydrophobic groups to the lipid phase and polar ionic segments to the aqueous phase. Thus, a significant relationship between emulsion stability with H_0 and protein solubility was reported (Nakai, 1983), which could be the reason of the improvement of 7S ESI after HUS (Fig. 3D). For 11S, on the other hand, ESI was very low, which may be attributed to the aggregated form of 11S in the standard buffer.

4. Conclusions

High intensity (400 W) ultrasound (HUS) did not significantly change the secondary structures of 7S and 11S fractions, but it altered their tertiary and quaternary structures as demonstrated by FT-Raman spectroscopy, SDS-PAGE and SH-group analysis. The effects of HUS on particle size, turbidity and emulsifying properties were more pronounced for the 7S fraction than the 11S fraction, which may be due to the extensive aggregation of 11S fraction proteins in pH 7.0 0.05 M Tris–HCl buffer (standard buffer). On the other hand, HUS effects on the physicochemical and functional properties of 7S could be attributed to partial dissociation of the aggregates. As the 11S fraction is highly aggregated in the standard buffer, further researches should be carried out to study the HUS effect on 11S in a more soluble state.

Acknowledgements

The authors would like to thank Natural Sciences & Engineering Research Council of Canada for financial support, Dr. Fred Rosell, Mr. John Jackson and Dr. David Plackett for technical support, and ADM company for the donation of 7B soy flour. The FT-Raman spectrometer and CD-polarimeter were provided through a grant from the Canadian Foundation for Innovation to the UBC Laboratory for Molecular Biophysics. The author Hao Hu would like to thank the Fundamental Research Funds for the Central Universities (No. 2662014BQ052), High Technology Research and Development Program of China (863 program, No. 2013AA102206) and China Scholarship Council (CSC) for financial support.

Appendix A. Supplementary data

Supplementary data related to this article can be found at http://dx.doi.org/10.1016/j.foodhyd.2014.11.004.

References

Adachi, M., Kanamori, J., Masuda, T., Yagasaki, K., Kitamura, K., Mikami, B., et al. (2003). Crystal structure of soybean 11S globulin: glycinin A3B4 homohexamer. *Proceedings of the National Academy of Sciences of the United States of America, 100*(12), 7395–7400.

Arzeni, C., Martínez, K., Zema, P., Arias, A., Pérez, O., & Pilosof, A. (2011). Comparative study of high intensity ultrasound effects on food proteins functionality. *Journal of Food Engineering, 108*(3), 463–472.

Bian, Y., Myers, D. J., Dias, K., Lihono, M. A., Wu, S., & Murphy, P. A. (2003). Functional properties of soy protein fractions produced using a pilot plant-scale process. *Journal of the American Oil Chemists' Society, 80*(6), 545–549.

Cameron, D. R., Weber, M. E., Idziak, E. S., Neufeld, R. J., & Cooper, D. G. (1991). Determination of interfacial areas in emulsions using turbidimetric and droplet size data: correction of the formula for emulsifying activity index. *Journal of Agricultural and Food Chemistry, 39*(4), 655–659.

Chandrapala, J., Zisu, B., Palmer, M., Kentish, S., & Ashokkumar, M. (2011). Effects of ultrasound on the thermal and structural characteristics of proteins in reconstituted whey protein concentrate. *Ultrasonics Sonochemistry, 18*(5), 951–957.

Chen, L., Chen, J., Ren, J., & Zhao, M. (2011). Effects of ultrasound pretreatment on the enzymatic hydrolysis of soy protein isolates and on the emulsifying properties of hydrolysates. *Journal of Agricultural and Food Chemistry, 59*(6), 2600–2609.

Chen, Y., & Ono, T. (2014). Protein particle and soluble protein structure in prepared soymilk. *Food Hydrocolloids, 39*, 120–126.

Faris, R. J., Wang, H., & Wang, T. (2008). Improving digestibility of soy flour by reducing disulfide bonds with thioredoxin. *Journal of Agricultural and Food Chemistry, 56*(16), 7146–7150.

Fukushima, D. (2001). Recent progress in research and technology on soybeans. *Food Science and Technology Research, 7*(1), 8–16.

Gordon, L., & Pilosof, A. M. R. (2010). Application of high-intensity ultrasounds to control the size of whey proteins particles. *Food Biophysics, 5*(3), 203–210.

Gülseren, İ., Güzey, D., Bruce, B. D., & Weiss, J. (2007). Structural and functional changes in ultrasonicated bovine serum albumin solutions. *Ultrasonics Sonochemistry, 14*(2), 173–183.

Hayakawa, S., & Nakai, S. (1985). Relationship of hydrophobicity and net charge to the solubility of milk and soy proteins. *Journal of Food Science, 50*(2), 486–491.

Hoshi, Y., & Yamauchi, F. (1983). Determination of sulfhydryl and disulfide contents of soybean 11S globulin and their change by lyophilization. *Agricultural and Biological Chemistry, 47*(11), 2435–2440.

Hou, D. H.-j., & Chang, S. K.-C. (2004a). Structural characteristics of purified glycinin from soybeans stored under various conditions. *Journal of Agricultural and Food Chemistry, 52*(12), 3792–3800.

Hou, H., & Chang, K. (2004b). Structural characteristics of purified β-conglycinin from soybeans stored under four conditions. *Journal of Agricultural and Food Chemistry, 52*(26), 7931–7937.

Hu, H., Fan, X., Zhou, Z., Xu, X., Fan, G., Wang, L., et al. (2013). Acid-induced gelation behavior of soybean protein isolate with high intensity ultrasonic pre-treatments. *Ultrasonics Sonochemistry, 20*(1), 187–195.

Hu, H., Li-Chan, E. C., Wan, L., Tian, M., & Pan, S. (2013). The effect of high intensity ultrasonic pre-treatment on the properties of soybean protein isolate gel induced by calcium sulfate. *Food Hydrocolloids, 32*(2), 303–311.

Hu, H., Wu, J., Li-Chan, E. C., Zhu, L., Zhang, F., Xu, X., et al. (2013). Effects of ultrasound on structural and physical properties of soy protein isolate (SPI) dispersions. *Food Hydrocolloids, 30*(2), 647–655.

Jambrak, A. R., Lelas, V., Mason, T. J., Kresic, G., & Badanjak, M. (2009). Physical properties of ultrasound treated soy proteins. *Journal of Food Engineering, 93*(4), 386–393.

Karki, B., Lamsal, B. P., Grewell, D., Pometto, A. L., Van Leeuwen, J., Khanal, S. K., et al. (2009). Functional properties of soy protein isolates produced from ultrasonicated defatted soy flakes. *Journal of the American Oil Chemists' Society, 86*(10), 1021–1028.

Kinsella, J. E. (1979). Functional properties of soy proteins. *Journal of the American Oil Chemists' Society, 56*(3), 242–258.

Li-Chan, E., Ismail, A., Sedman, J., & van de Voort, F. (2002). Vibrational spectroscopy of food and food products. In J. M. Chalmers, & P. R. Griffiths (Eds.), *Handbook of vibrational spectroscopy* (pp. 1–33). West Sussex: Wiley & Sons Ltd.

Liu, Z. S., & Chang, S. K. C. (2004). Effect of soy milk characteristics and cooking conditions on coagulant requirements for making filled tofu. *Journal of Agricultural and Food Chemistry, 52*, 3405–3411.

Madadlou, A., Mousavi, M. E., Emam-Djomeh, Z., Ehsani, M., & Sheehan, D. (2009). Comparison of pH-dependent sonodisruption of re-assembled casein micelles by 35 and 130 kHz ultrasounds. *Journal of Food Engineering, 95*(3), 505–509.

Martini, S., Potter, R., & Walsh, M. (2010). Optimizing the use of power ultrasound to decrease turbidity in whey protein suspensions. *Food Research International, 43*(10), 2444–2451.

Maruyama, N., Adachi, M., Takahashi, K., Yagasaki, K., Kohno, M., Takenaka, Y., et al. (2001). Crystal structures of recombinant and native soybean β-conglycinin β homotrimers. *European Journal of Biochemistry, 268*, 3595–3604.

Maruyama, N., Sato, R., Wada, Y., Matsumura, Y., Goto, H., Okuda, H., et al. (1999). Structure–physicochemical function relationships of soybean b-conglycinin constituent subunits. *Journal of Agricultural and Food Chemistry, 47*, 5278–5284.

Moon, S.-Y., & Li-Chan, E. C. (2007). Assessment of added ingredient effect on interaction of simulated beef flavour and soy protein isolate by gas chromatography, spectroscopy and descriptive sensory analysis. *Food Research International, 40*(10), 1227–1238.

Nagano, T., Hirotsuka, M., Mori, H., Kohyama, K., & Nishinari, K. (1992). Dynamic viscoelastic study on the gelation of 7 S globulin from soybeans. *Journal of Agricultural and Food Chemistry, 40*(6), 941–944.

Nakai, S. (1983). Structure–function relationships of food proteins: with an emphasis on the importance of protein hydrophobicity. *Journal of Agricultural and Food Chemistry, 31*(4), 676–683.

Nishinari, K., Fang, Y., Guo, S., & Phillips, G. O. (2014). Soy protein: a review on composition, aggregation and emulsification. *Food Hydrocolloids, 39*, 301–318. http://dx.doi.org/10.1016/j.foodhyd.2014.01.013.

Pearce, K. N., & Kinsella, J. E. (1978). Emulsifying properties of proteins: evaluation of a turbidimetric technique. *Journal of Agricultural and Food Chemistry, 26*(3), 716–723.

Shen, L., & Tang, C. H. (2012). Microfluidization as a potential technique to modify surface properties of soy protein isolate. *Food Research International, 48*(1), 108–118.

Shimada, K., & Cheftel, J. C. (1988). Determination of sulfhydryl groups and disulfide bonds in heat-induced gels of soy protein isolate. *Journal of Agricultural and Food Chemistry, 36*(1), 147–153.

Stathopulos, P. B., Scholz, G. A., Hwang, Y. M., Rumfeldt, J. A. O., Lepock, J. R., & Meiering, E. M. (2004). Sonication of proteins causes formation of aggregates that resemble amyloid. *Protein Science, 13*(11), 3017–3027.

Tang, C. H., Chen, L., & Foegeding, E. A. (2011). Mechanical and water-holding properties and microstructures of soy protein isolate emulsion gels induced by $CaCl_2$, GDL and transglutaminase: influence of thermal treatments before and/or after emulsification. *Journal of Agricultural and Food Chemistry, 59*(8), 4071–4077.

Tang, C. H., Sun, X., & Foegeding, E. A. (2011). Modulation of physicochemical and conformational properties of kidney bean vicilin (phaseolin) by glycation with glucose: implications for structure–function relationships of legume vicilins. *Journal of Agricultural and Food Chemistry, 59*(18), 10114–10123.

Tang, C. H., Wang, X. Y., Yang, X. Q., & Li, L. (2009). Formation of soluble aggregates from insoluble commercial soy protein isolate by means of ultrasonic treatment and their gelling properties. *Journal of Food Engineering, 92*(4), 432–437.

Tezuka, M., Yagasaki, K., & Ono, T. (2004). Changes in characters of soybean glycinin groups I, IIa, and IIb caused by heating. *Journal of Agricultural and Food Chemistry, 52*(6), 1693–1699.

Thanh, V. H., & Shibasaki, K. (1976). Major proteins of soybean seeds. A straightforward fractionation and their characterization. *Journal of Agricultural and Food Chemistry, 24*(6), 1117–1121.

Wu, S., Murphy, P. A., Johnson, L. A., Fratzke, A. R., & Reuber, M. A. (1999). Pilot-plant fractionation of soybean glycinin and β-conglycinin. *Journal of the American Oil Chemists' Society, 76*(3), 285–293.

Zhang, H., Li, L., & Mittal, G. (2010). Effects of high pressure processing on soybean beta-conglycinin. *Journal of Food Process Engineering, 33*(3), 568–583.

Zheng, L., & Sun, D.-W. (2006). Innovative applications of power ultrasound during food freezing processes—a review. *Trends in Food Science & Technology, 17*(1), 16–23.

Zhu, J. H., & Yang, X. Q. (2010). Effect of sonication on soy protein (in Chinese) *Cereals and Oil Processing, 7*, 39–42.

Zisu, B., Bhaskaracharya, R., Kentish, S., & Ashokkumar, M. (2010). Ultrasonic processing of dairy systems in large scale reactors. *Ultrasonics Sonochemistry, 17*(6), 1075–1081.